



Investigating Skin Cancer Diagnosis Using a Webcam-based Microcontroller System

Raymond Kim ^{a*}

^a *Biomedical Computer Sciences Division, STEM Science Center, 111 Charlotte Place/Englewood
Cliffs, NJ 07632, USA.*

Author's contribution

The sole author designed, analysed, interpreted and prepared the manuscript.

Article Information

DOI: 10.56557/JIRMEPS/2024/v19i18624

Open Peer Review History:

This journal follows the Advanced Open Peer Review policy. Identity of the Reviewers, Editor(s) and additional Reviewers, peer review comments, different versions of the manuscript, comments of the editors, etc are available here: <https://prh.ikpress.org/review-history/11992>

Original Research Article

Received: 25/01/2024

Accepted: 29/03/2024

Published: 03/04/2024

ABSTRACT

Skin cancer can spread fast to nearby tissue and other parts of the human body if it's not diagnosed early. Most are curable only if skin cancer is found and treated in the early stages. Therefore, it's essential to seek a casual way of early diagnosis. This paper assesses a prototype system for skin cancer detection using an Arduino with an ArduCam Mega 5MP, benchmarked against smartphone diagnosis. Bandpass filters capture skin images at red (650 nm), green (532 nm), and blue (450 nm) wavelengths, measuring reflectance values. The approach aims to quantitatively determine skin melanin, oxyhemoglobin, and deoxyhemoglobin levels, aiding in various skin lesions' diagnosis. Evaluation involves comparing pixel reflectance values of images taken by smartphones and the prototype using a 3D mesh grid. Applying the modified Lambert-Beer law to reflectance values of moles, pimples, scars, scabs, and traces predicts relative levels of skin components. The system shows an 87% match with the smartphone standard, demonstrating high reliability. Further study might be needed to clarify the confirmation with clinical cases.

*Corresponding author: E-mail: Rkim@STEMsc.org;

Keywords: Lambert-beer law; reflectance value; skin cancer diagnosis; skin melanin; webcam based microcontroller system.

1. INTRODUCTION AND HYPOTHESIS

Skin cancer, particularly melanoma, requires early detection for effective treatment, with survival rates dropping significantly once it spreads [1,2]. Despite advancements in diagnosis and treatment since the 18th century, the disease's varied appearances complicate early detection. Traditional methods, such as dermoscopy, have limitations, leading to the exploration of more accessible diagnostic tools like microcontroller systems, which promise to enhance early detection efforts without requiring direct consultations [3,4].

Early detection of melanoma is crucial for survival, with rates dropping from nearly 100% to 35% once it spreads [5]. Traditional diagnostics, relying on dermatologists' expertise, such as dermoscopy, have their limits, particularly in early detection, despite a high sensitivity. Technological advances have prompted the search for alternative methods, such as algorithm-based diagnostics, but these still lack accessibility and require face-to-face consultations [6]. This highlights the demand for more accessible, reliable diagnostic tools, leading to innovative approaches like using a microcontroller system for early skin cancer detection.

The history of skin cancer dates all the way back to the 5th century BC. This was when the first record of melanoma, a type of skin cancer, was recorded by Hippocrates, and it was described as black tumors [7]. In 1787, Jack Hunter became the first person to diagnose and operate on a person with melanoma cancer, the deadliest skin cancer at the time. Rene Laenec was the first to distinguish melanoma as a disease separate from others in 1804 [8]. As time passed, more knowledge was gained about melanoma. In the 20th century, doctors diagnosed skin cancer in two main ways. The first method was through the diagnosis of lymphatic disorders. William Handley used the "lymph angioplasty" method, which used silk threads subcutaneously to create a conduit for lymphatic drainage [9]. However, this method was soon abandoned due to postoperative infections and spontaneous ejection of the foreign material [10]. The second way 20th-century doctors diagnosed skin cancer was through prophylaxis, which was used by Herbert

Snow [11]. This eventually led to the technology that exists today, the Vectra WB180 [12]. However, dermoscopies are still not 100% reliable today, and diagnosing skin cancer early is still a challenge even with dermoscopy [13]. Despite this, the diagnosis of skin cancer today is more advanced than ever. But, we would like to introduce a new testing method for skin cancer that might provide a more accessible method for people to use at home as a cost-effective diagnostic test. Traditionally, the government has approved many of these skin cancer diagnosis devices. Similarly, the systems and designs we might develop in the future must also be approved. To get FDA permission for a medical device, the inventor must first classify the device into three classes: I, II, or III. Classes I, II, and III are separated because Class I is reserved for low-risk devices. The applicant would have to develop a prototype of the device to test for ethicality and functionality. After the prototype may be created, they would need to apply to the device depending on its class. They would need to fulfill both FDA validation and verification requirements to apply. After, they would need to wait for the FDA to review and approve their device. However, even after the applicant receives FDA approval, they must maintain FDA compliance [14].

The discussion on melanoma diagnosis emphasizes the significance of melanin, deoxyhemoglobin, and oxyhemoglobin in differentiating melanoma from benign skin conditions [15]. Melanoma lesions exhibit increased melanin levels, while changes in blood supply, influenced by angiogenesis, affect oxyhemoglobin and deoxyhemoglobin levels. The balance between these components offers insights into melanoma metabolic activity, with the relative ratio of oxyhemoglobin to deoxyhemoglobin acting as a potential melanoma indicator [16].

Building on this foundation, the aim is to enhance melanoma detection through a prototype system designed for early-stage skin cancer diagnosis. This system leverages optical RGB images and a band-filter lens to measure skin reflectance accurately [17]. Applying the Beer-Lambert equation quantifies the concentrations of hemoglobin, deoxyhemoglobin, and melanin. This approach facilitates a more accessible means for individuals to evaluate the likelihood of

skin cancer, encouraging early medical consultation based on preliminary findings [18].

Our technique might be widespread in the future for home diagnosis and machine-learning devices to be mass-produced and for more people to use these different devices to reduce the rates of skin cancer deaths worldwide. Ultimately, this actualizes the optimal individualization of treatment for each patient and the detection of various types of skin cancer at an early stage [19]. In addition, these technological advances will be optimized for early diagnosis of cancers, especially melanoma, which is a potentially aggressive cancer with a high tendency for lymphatic and visceral metastasis [20]. Home diagnosis is considered the final destination of cancer diagnosis technology, and it may greatly help those living in remote areas and areas without ready access to healthcare [21]. Through detection using mobile devices, patients living in geographically remote areas can take advantage of teledermatology services or possibly even be trained to use Mobile Teledermoscopy (MTD) as an adjunct to Skin Self-Examination (SSE) [22]. Thinking intuitively about these methods and technologies should also help to reduce the morbidity and mortality of skin cancer.

From the point of accuracy side, 3D full-body imaging in hospitals is far superior to home diagnosis. A further extension of the dermoscopy method is the 3D total body photography imaging system, which captures multiple snapshots to create a 3D model of the patient's body [23]. Vectra WB180, installed in The Waldman Melanoma and Skin Cancer Center, located in New York City, takes 92 photos of the patient and then compiles all of these photos into one 3D image of the patient. This 3D image shows the growth or lesions by size, shape, and color of the skin cells [24]. However, despite its high accuracy, it is not accessible. Thus, in the early stages of cancer, it is improbable that the patient decides to take a complete body picture through this machine.

To address this accessibility problem, companies worldwide seek reliable and accurate cell phone-based biopsies for skin and skin cancer [25]. Cell phone-based biopsies need a high-resolution camera on the phone in order for the picture to capture every part of the skin [26].

Together, these insights and technological advancements highlight the potential of using

specific wavelengths, imaging techniques, and quantitative measures to improve early skin cancer detection. Further research and development in this area promise to yield effective, noninvasive diagnostic tools that will significantly impact patient outcomes by enabling timely treatment of melanoma.

To test the system's effectiveness, the experiment will use optical images from a smartphone with a band-filter lens, serving as a benchmark. These images will be assessed using the modified Beer-Lambert law, supported by studies validating smartphone images for skin cancer diagnosis. The aim is to compare melanin, deoxyhemoglobin, and oxyhemoglobin levels in the images' Regions of Interest (ROIs) with those taken by the system to evaluate variance and diagnostic accuracy for skin cancer.

2. MEDHODS

2.1 Experimental Components

ASCD(Arduino skin cancer diagnosis) System is an embedded ArduCam Mega 5MP and Arduino Uno to capture Skin ROI images. The ArduCam Mega 5MP model features a powerful 5MP CMOS image sensor for enhanced image-capturing accuracy. The ASCD System aims to use RGB color channels to detect and differentiate between moles and melanoma cells, employing OpenCV for image processing. Subsequently, All images are saved through the ArduCam Mega (v2.0) - (updated 2023/04/24 - b0cb3b1) before image processing. To assess the accuracy of the ASCD System, images of various body parts were captured, referred to as the ROI (Region of Interest). This prototype aims to represent essential parameters for melanoma diagnosis—melanin, deoxyhemoglobin, and hemoglobin—within the skin tissue of the ROI as 3D images. If it's possible to measure the concentrations of these three parameters in specific normal skin areas (moles, pimples, scabs), it indicates the potential of the ASCD System for melanoma detection.

In this experiment, the smartphone is used as the gold standard to compare the diagnostic capabilities of the ASCD System. Smartphones' optical skin cancer diagnosis ability has already been verified and is being used for commercial purposes. All experiments are conducted identically with both the smartphone and the ASCD System.

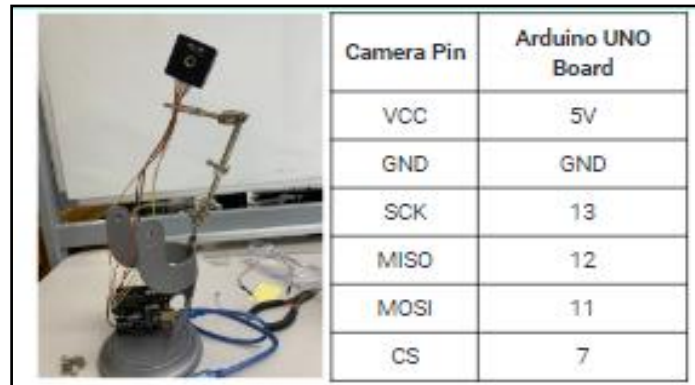


Fig. 1. ASCD system (left), Pin connection with Arduino UNO and Ardu Cam Mega(Right)



	Galaxy Note 10+	Arducam Mp5
appearance		
Resolution	4K	2592 x 1944
Focal length[mm]	27	3.3
Dimension[mm]	26	33x33x17

Fig. 2. Comparative Specification of Smartphone and Arducam Mega 5mp

image: www.comptones.com Cameng-Gel-No1011155 Nipadam.com/Aduino-SlamaVEGA-SI 1 MEGA-SM

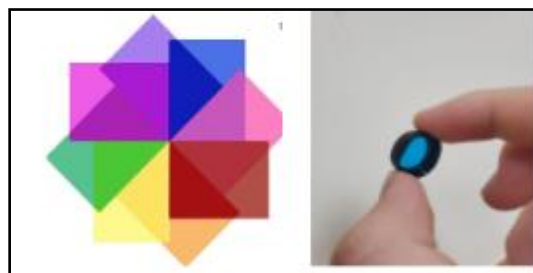


Fig. 3. Red,Green, Blue band filter film SAKOLLA Transparent Color Correction Lighting Gel Filter[Left] Color Cap for ASCD

maspx/www.com/

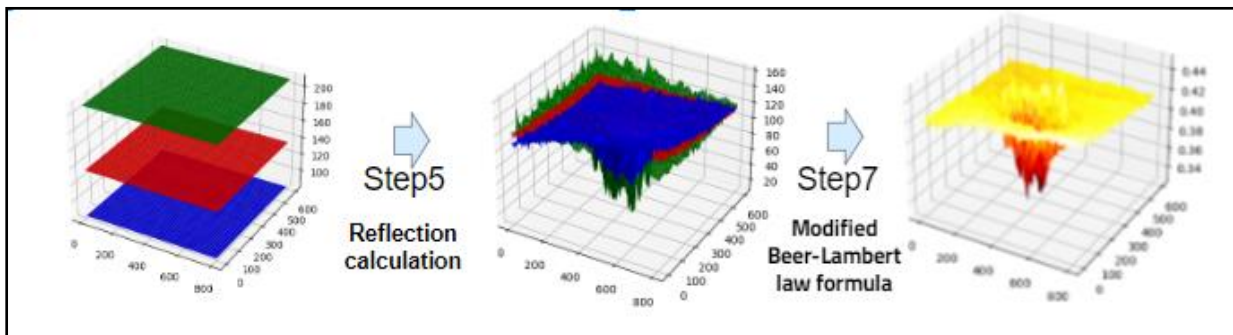


Fig. 4. Schematic Representation of Converting Reflectance Values from RGB Channels into an Optical Color Map

Three color caps are used when shooting the Region of Interest (ROI). These color caps are equipped with band filter color transparent paper that filters light at 650 nm, 532nm, and 405 nm wavelengths, respectively, and are installed at the front. Their diameter is about 35mm.

2.2 Our Step-wise Procedure

1. Setup & Calibration: Ensure the ASCD System is ready and attach a color cap to the ArduCam Mega 5MP camera. Capture a calibration image of a white paper with the red color cap to create a reference image (img white red).

3. Capture Normal Skin Images: With the red cap, capture three photos of normal skin without distinct features. Capture the normal skin near the ROI, which will be photographed later. Use the cv2.imread method to specify the pixel values as an array, saving this array as img_normal_red.

4. Feature and ROI Capture: Using the red color cap, capture the skin feature (dot) as the ROI. Ensure each feature is captured with all color caps and save these images for analysis. Use the cv2.imread method to specify the pixel values as an array, saving this array as img_sample_red.

5. Reflectance Calculation: Insert the following formula into the algorithm to calculate reflectance. All operations must be performed as array calculations:

$$\begin{aligned} reflect_i_red &= img_sample_red/img_white_red \\ reflect_bg_red &= img_normal_red/img_white_red \\ reflect_hat_red &= reflect_i_red/reflect_bg_red \end{aligned}$$

6. Repeat Steps 2-5 for other color caps to obtain reflect_hat_green and reflect_hat_blue.

7. Data Analysis: Use the modified Beer-Lambert law formula to calculate the concentration of oxyhemoglobin (HbO₂), deoxyhemoglobin (Hb), and melanin (m) in the skin based on the reflectance values obtained from the images. The formulas are as follows:

$$\begin{aligned} HbO_2 &= -0.024 \ln(reflect_hat_blue) - 0.033 \ln(reflect_hat_green) + 0.145 \ln(reflect_hat_red) \\ Hb &= 0.057 \ln(reflect_hat_blue) - 0.024 \ln(reflect_hat_green) - 0.128 \ln(reflect_hat_red) \\ m &= -0.806 \ln(reflect_hat_blue) + 0.408 \ln(reflect_hat_green) - 0.806 \ln(reflect_hat_red) \end{aligned}$$

Citation: Delpy, D. T., et al. (1988). Physics in Medicine & Biology.

8. Repeat Steps 2-7 for different ROIs. Display all analyzed images using the colormap "hot" in a surface mesh 3D map.

9. Smartphone Comparison: Follow the same method to Repeat Steps 1-8 using a smartphone instead of the ASCD System.

10. Verification and Comparison: Validate that the hemoglobin, deoxyhemoglobin, and melanin concentrations in each ROI match the findings presented in professional articles. Confirm that the biometric information of moles, pimples, and scabs in normal skin tissue matches the research descriptions. Perform a t-test with the dataset of all reflectance array data to statistically compare the reflection values obtained from the smartphone and the ASCD System.

3. RESULTS AND DISCUSSION

3.1 Mole Images and Graphic Interpretation

The analysis of melanin, oxyhemoglobin (HbO₂), and deoxyhemoglobin (Hb) in a normal mole through RGB channel reflectance ratios shows distinct patterns, as seen in Fig. 5. Melanin concentration peaks in the mole area due to its light-absorbing property. In contrast, HbO₂ and Hb display opposite values, aligning with their theoretical opposition. The area surrounding the mole shows a consistent distribution of HbO₂ and Hb, unlike the pronounced peak. Smartphone photography failed to confirm smoother peak variations, whereas ASCD outlined peak shapes but didn't capture the normal skin tissue's uniform distribution around them. Additionally, HbO₂ and Hb values weren't exact opposites, indicating noise. The Hb peak was unclear and appeared smeared. Nonetheless, the precise melanin peak representation suggests the potential to detect increased melanin in melanoma.

3.2 Pimple Images and Graphic Interpretation

In pimple-affected areas, as in Fig. 6 an inflammatory response leads to increased blood flow, elevating HbO₂ and Hb levels. In contrast, melanin levels remain relatively unaffected due to pimples' weak association with melanin increase. Smartphone imaging shows lower reflectance values, and while ASCD presents lower values for HbO₂, it more accurately reflects the high levels of HbO₂ and Hb associated with

pimples' physiological characteristics. Despite some discrepancies in reflectance distribution, both methods indicate elevated HbO₂, with ASCD offering a slightly more accurate depiction of HbO₂ and Hb levels in pimples.

Melanin, HbO₂, and Hb distribution in a normal scab (Fig. 7) reflect the physiological changes during wound healing. The formation of a scab results from the coagulation of blood components, which does not directly affect melanin concentration, but melanin production can increase in the skin surrounding the scab. This could be a response from the skin to protect itself from the wound. Both smartphones and the ASCD have been shown to represent this melanin production effectively. Meanwhile, the formation of new blood vessels for wound healing increases the concentrations of HbO₂ and Hb, particularly noticeable in the area with a scab.

3.3 Scar Images and Graphic Interpretation

The comparison between smartphone and ASCD device images for moles, pimples, and scabs

shows no significant differences in melanin, HbO₂, and Hb levels, with most p-values indicating no statistical significance. An average p-value of approximately 25.38% suggests a 74.62% likelihood of no significant difference between the two imaging methods, indicating their interchangeability for diagnostic and monitoring purposes, the difference between the images taken with smartphones and ASCD devices.

3.4 Statistical Analysis

The comparison between smartphone and ASCD device images for moles, pimples, and scabs shows no significant differences in melanin, HbO₂, and Hb levels, with most p-values indicating no statistical significance. An average p-value of approximately 25.38% suggests a 74.62% likelihood of no significant difference between the two imaging methods. This shows their interchangeability for diagnostic and monitoring purposes—the difference between the images taken with smartphones and ASCD devices.

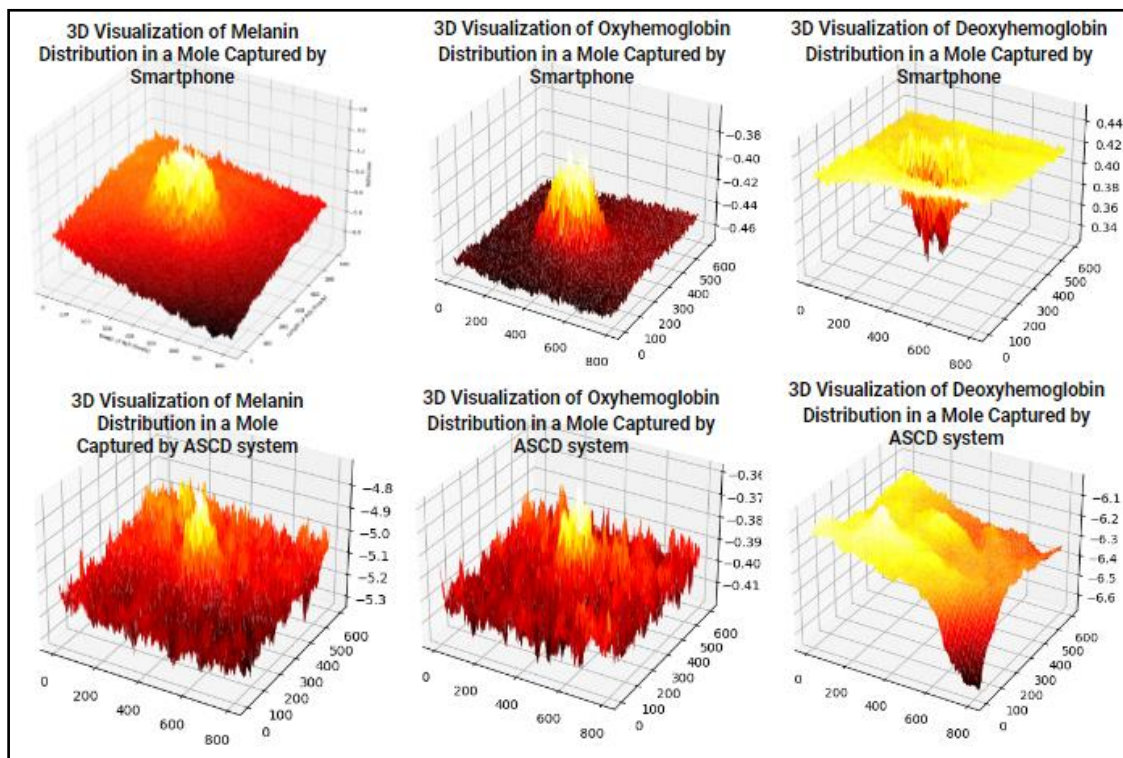


Fig. 5. Comparative 3D Visualization of Melanin, Oxyhemoglobin, and Deoxyhemoglobin Distributions in a Mole: Smartphone vs. ASCD System[x: Width of ROI, y: Length of ROI, z: Relative concentration parameter]

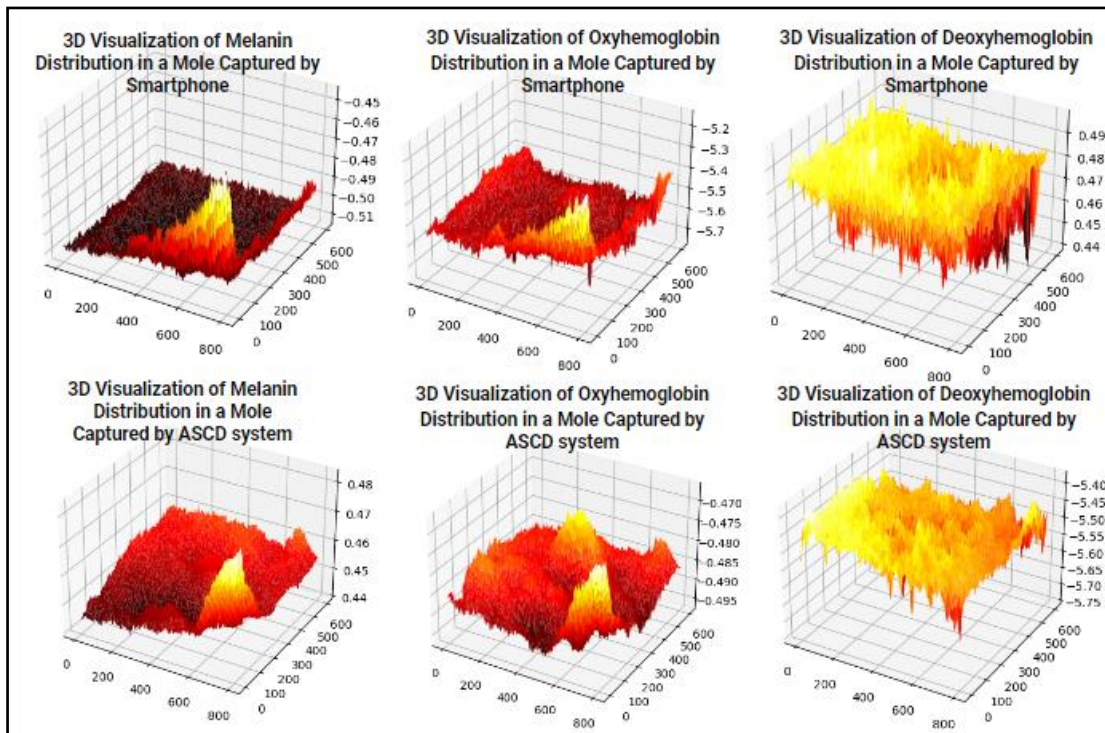


Fig. 6. Comparative 3D Visualization of Melanin, Oxyhemoglobin, and Deoxyhemoglobin Distributions in a Mole: Smartphone vs. ASCD System [x: Width of ROI, y: Length of ROI, z: Relative concentration parameter]

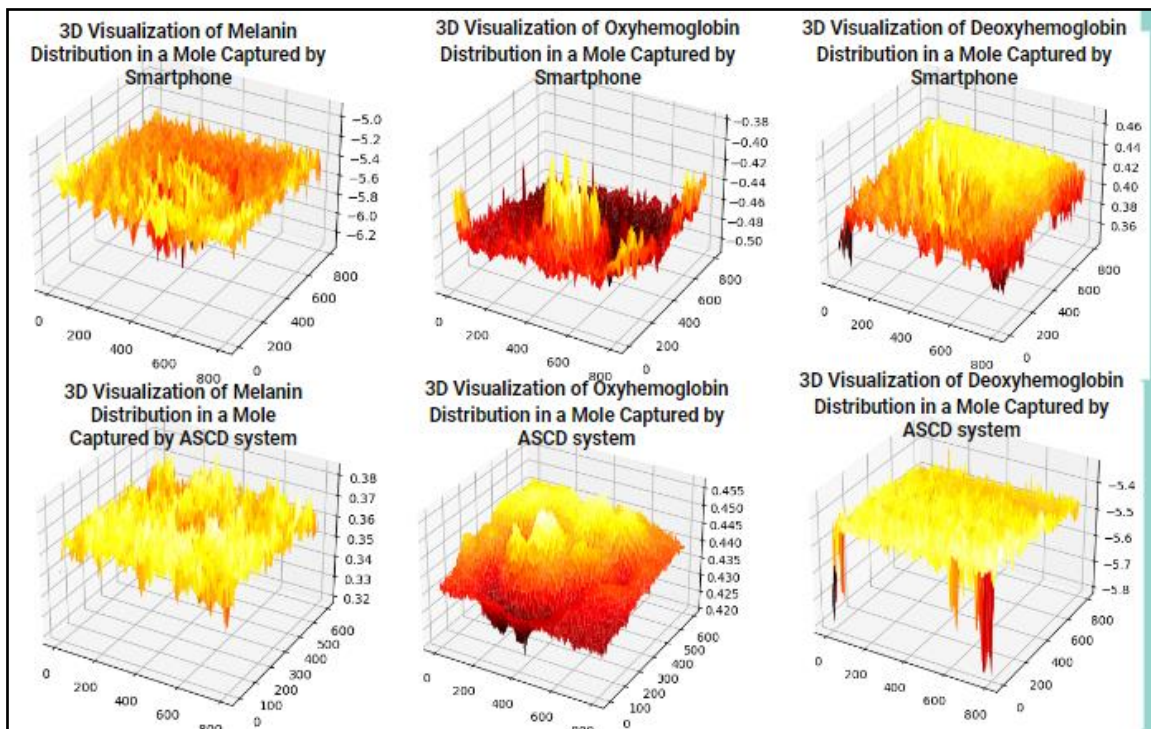


Fig. 7. Comparative 3D Visualization of Melanin, Oxyhemoglobin, and Deoxyhemoglobin Distribution in Scars: Smartphone vs. ASCD System [x: Width of ROI, y: Length of ROI, z: Relative concentration parameter]

Table 1. T-test Statistical Analysis of Reflectance Ratios: Comparing Smartphone and ASCD System in Imaging Skin Conditions

ROI with System	t	df	P-value	SE	Difference
Mole M	-0.7779	959998	0.4365	0.000454	No difference
Mole HbO2	-0.9361	959998	0.3491	2.8890 x 10 ⁻⁵	No difference
Mole Hb	-1.7972	959998	0.0723	2.8882 x 10 ⁻⁵	difference
pimple Melanin	1.2551	959998	0.2094	0.000248	No difference
pimple HbO2	1.0272	959998	0.3042	2.1951 x 10 ⁻⁵	No difference
pimple Hb	-1.0695	959998	0.2848	2.4074 x 10 ⁻⁵	No difference
scab Melanin	-1.1917	959998	0.2333	0.000265	No difference
scab HbO2	-1.3754	959998	0.1690	2.4611 x 10 ⁻⁵	No difference
scab Hb	1.2122	959998	0.2254	3.5291 x 10 ⁻⁵	No difference

This comprehensive analysis across various skin conditions—moles, pimples, and scabs—reveals significant insights into the diagnostic capabilities of smartphone and Advanced Skin Condition Diagnosis (ASCD) devices. It highlights the intricacies of melanin, oxyhemoglobin (HbO₂), and deoxyhemoglobin (Hb) distributions under different skin conditions, offering a window into the physiological processes at play.

For moles, the analysis underscores the elevated melanin concentration, a characteristic feature that both imaging methods can capture, albeit with nuances in their accuracy. The expected theoretical patterns for HbO₂ and Hb concentrations demonstrate the challenge of capturing exact physiological responses, with noise interference impacting the clarity of results. This suggests a nuanced approach is necessary when interpreting such data, especially in the context of melanoma detection.

In the case of pimples, the analysis points to an increase in HbO₂ and Hb levels due to the inflammatory response, a condition that smartphones and ASCD devices can detect. However, the device's ability to accurately reflect the elevated levels of these markers varies, indicating a need for careful consideration of the chosen method for specific diagnostic purposes.

The examination of scabs reveals how smartphones and ASCD devices capture the physiological changes of wound healing, such as increased melanin production around the scab and the formation of new blood vessels. The data suggests both devices can reflect these changes, with nuances in their ability to delineate between normal skin and scab tissue, particularly for HbO₂ and Hb concentrations.

The statistical analysis, indicating no significant difference in the performance of smartphones and ASCD devices across a range of p-values, suggests a high degree of interchangeability between these imaging methods for diagnosing and monitoring skin conditions. This conclusion, supported by an average p-value translating into a 74.62% likelihood of no significant difference, underscores the potential of using readily available smartphone technology alongside more advanced devices in dermatological assessments.

Ultimately, this analysis highlights the potential and limitations of current imaging technology in capturing key physiological indicators across different skin conditions and opens the door for further research. It calls for developing more refined imaging techniques and algorithms that can improve the accuracy and reliability of skin condition diagnosis, leveraging the ubiquity and accessibility of smartphone technology to enhance patient care in dermatology.

4. CONCLUSION

This study explores the diagnostic capabilities of smartphones & ASCD devices by analyzing melanin, HbO₂, & Hb distributions in skin conditions like moles, pimples, & scabs. For moles, both methods captured higher melanin concentration but faced challenges in capturing the theoretical patterns of HbO₂ & Hb distributions, suggesting noise interference impacts accuracy. The analysis of pimples highlighted an increase in HbO₂ & Hb levels due to the inflammatory response, with ASCD showing a superior ability to distinguish these changes more accurately than smartphones. In the case of scabs, both smartphones & ASCD effectively captured physiological changes

associated with wound healing, like increased melanin production around the scab & the formation of new blood vessels. However, there were subtle differences in their capabilities to capture HbO₂ & Hb concentrations, an important consideration when comparing device performance. Statistical analysis showed no significant difference in performance between smartphones & ASCD, suggesting the two imaging methods can be interchangeably used for the diagnosis & monitoring of skin conditions. In conclusion, ASCD has performed satisfactorily enough to replace the diag capabilities of commercially available smartphones potentially. This signifies a promising direction for the future of dermatological assessments, indicating that ASCD can be considered a viable alternative to conventional smartphone-based diagnostics.

CONSENT AND ETHICAL APPROVAL

It is not applicable.

COMPETING INTERESTS

Author has declared that no competing interests exist.

REFERENCES

1. Davis LE, Shalin SC, Tackett AJ. Current state of melanoma diagnosis and treatment. *Cancer Biol Ther.* 2019;20(11):1366-1379. DOI: 10.1080/15384047.2019.1640032. Epub 2019 Aug 1. PMID: 31366280 PMID: PMC6804807
2. Rigel, DS, Carucci, JA. Malignant melanoma: prevention, early detection and treatment in the 21st century. *CA-A Cancer Journal For Clinicians.* 2000;50(4):215-236.
3. Reddy S, Shaheed A, Patel R. Artificial intelligence in dermoscopy: Enhancing diagnosis to distinguish benign and malignant skin lesions. *Cureus.* 2024 Feb 21;16(2):e54656. DOI: 10.7759/cureus.54656 PMID: 38523958 PMID: PMC10959827
4. Sonthalia S, Yumeen S, Kaliyadan F. Dermoscopy overview and extradiagnostic applications. [Updated 2023 Aug 8]. In: *StatPearls. Treasure Island (FL): StatPearls Publishing; 2024 Jan-* Available: <https://www.ncbi.nlm.nih.gov/books/NBK537131/>
5. Voss RK, Woods TN, Cromwell KD, Nelson KC, Cormier JN. Improving outcomes in patients with melanoma: Strategies to ensure an early diagnosis. *Patient Relat Outcome Meas.* 2015 Nov 6;6:229-42. DOI: 10.2147/PROM.S69351 PMID: 26609248 PMID: PMC4644158
6. Bohr A, Memarzadeh K. The rise of artificial intelligence in healthcare applications. *Artificial Intelligence in Healthcare.* 2020;25-60. DOI: 10.1016/B978-0-12-818438-7.00002-2 Epub 2020 Jun 26. PMID: PMC7325854.
7. Rebecca VW, Sondak VK, Smalley KS. A brief history of melanoma: from mummies to mutations. *Melanoma Res.* 2012 Apr;22(2):114-22. DOI: 10.1097/CMR.0b013e328351fa4d PMID: 22395415 PMID: PMC3303163
8. Richard A, Scolyer, Georgina V. Long, John F. Thompson. Evolving concepts in melanoma classification and their relevance to multidisciplinary melanoma patient care, *Molecular Oncology.* 2011;5(2):124-136. ISSN 1574-7891 Available: <https://doi.org/10.1016/j.molonc.2011.03.002>
9. Cheon H, Gelvosa MN, Kim SA, Song HY, Jeon JY. Lymphatic channel sheet of polydimethylsiloxane for preventing secondary lymphedema in the rat upper limb model. *Bioeng Transl Med.* 2022 Jul 5;8(1):e10371. DOI: 10.1002/btm2.10371 PMID: 36684082 PMID: PMC9842043
10. van Schaik CJ, Boer LL, Draaisma JMT, van der Vleuten CJM, Janssen JJ, Fütterer JJ, Schultze Kool LJ, Klein WM. The lymphatic system throughout history: From hieroglyphic translations to state of the art radiological techniques. *Clin Anat.* 2022 Sep;35(6):701-710. DOI: 10.1002/ca.23867. Epub 2022 Apr 9 PMID: 35383381 PMID: PMC9542037
11. Davis LE, Shalin SC, Tackett AJ. Current state of melanoma diagnosis and treatment. *Cancer Biol Ther.* 2019;20(11):1366-1379.

- DOI: 10.1080/15384047.2019.1640032.
Epub 2019 Aug 1
PMID: 31366280
PMCID: PMC6804807
12. Albert T. Young, Niki B. Vora, Jose Cortez, Andrew Tam, Yildiray Yeniay, Ladi Afifi, Di Yan, Adi Nosrati, Andrew Wong, Arjun Johal, Maria L. Wei, The role of technology in melanoma screening and diagnosis, pigment cell & melanoma research, special issue: Proceedings of the International Pigment Cell Conference 2020, March 2021;288-300.
 13. Dinnes J, Deeks JJ, Chuchu N, Ferrante di Ruffano L, Martin RN, Thomson DR, Wong KY, Aldridge RB, Abbott R, Fawzy M, Bayliss SE, Grainge MJ, Takwoingi Y, Davenport C, Godfrey K, Walter FM, Williams HC; Cochrane skin cancer diagnostic test accuracy group. Dermoscopy, with and without visual inspection, for diagnosing melanoma in adults. *Cochrane Database Syst Rev*. 2018 Dec 4;12(12):CD011902.
DOI: 10.1002/14651858.CD011902.pub2
PMID: 30521682
PMCID: PMC6517096
 14. Hasan N, Nadaf A, Imran M, Jiba U, Sheikh A, Almalki WH, Almuji SS, Mohammed YH, Kesharwani P, Ahmad FJ. Skin cancer: Understanding the journey of transformation from conventional to advanced treatment approaches. *Mol Cancer*. 2023 Oct 6;22(1):168.
DOI: 10.1186/s12943-023-01854-3
PMID: 37803407
PMCID: PMC10559482
 15. Hessler M, Jalilian E, Xu Q, Reddy S, Horton L, Elkin K, Manwar R, Tsoukas M, Mehregan D, Avnaki K. Melanoma biomarkers and their potential application for *In vivo* diagnostic imaging modalities. *Int J Mol Sci*. 2020 Dec 16;21(24):9583.
DOI: 10.3390/ijms21249583
PMID: 33339193
PMCID: PMC7765677
 16. Carrié L, Virazels M, Dufau C, Montfort A, Levade T, Ségui B, Andrieu-Abadie N. New Insights into the Role of Sphingolipid Metabolism in Melanoma. *Cells*. 2020 Aug 26;9(9):1967.
DOI: 10.3390/cells9091967
PMID: 32858889
PMCID: PMC7565650
 17. Leon, Raquel, Martinez-Vega, Beatriz, Fabelo, Himar, Ortega, Samuel, Melian, Veronica, Castaño, Irene, Carretero, Gregorio, Almeida, Pablo, Garcia, Aday, Quevedo Gutiérrez, Eduardo, Hernandez, Javier, Clavo, Bernardino, Marrero Callico, Gustavo. Non-invasive skin cancer diagnosis using hyperspectral imaging for *In situ* clinical support. *Journal of Clinical Medicine*. 2020;9:1662.
DOI: 10.3390/jcm9061662
 18. Oshina I, Spigulis J. Beer-Lambert law for optical tissue diagnostics: Current state of the art and the main limitations. *J Biomed Opt*. 2021 Oct;26(10):100901.
DOI: 10.1117/1.JBO.26.10.100901
PMID: 34713647
PMCID: PMC8553265
 19. Jung JM, Cho JY, Lee WJ, Chang SE, Lee MW, Won CH. Emerging minimally invasive technologies for the detection of skin cancer. *J Pers Med*. 2021 Sep 24;11(10):951.
DOI: 10.3390/jpm11100951
PMID: 34683091
PMCID: PMC8538732
 20. Higgins H, Nakhla A, Lotfalla A, Khalil D, Doshi P, Thakkar V, Shirini D, Bebawy M, Ammari S, Lopci E, Schwartz LH, Postow M, Dercle L. Recent advances in the field of artificial intelligence for precision medicine in patients with a diagnosis of metastatic cutaneous melanoma. *Diagnostics (Basel)*. 2023 Nov 20;13(22):3483.
DOI: 10.3390/diagnostics13223483
PMID: 37998619
PMCID: PMC10670510
 21. Elder AJ, Alazawi H, Shafaq F, Ayyad A, Hazin R. Teleoncology: Novel approaches for improving cancer care in North America. *Cureus*. 2023 Aug 16;15(8):e43562.
DOI: 10.7759/cureus.43562
PMID: 37719501
PMCID: PMC10502915
 22. Lee KJ, Finnane A, Soyer HP. Recent trends in teledermatology and teledermoscopy. *Dermatol Pract Concept*. 2018 Jul 31;8(3):214-223.
DOI: 10.5826/dpc.0803a13
PMID: 30116667
PMCID: PMC6092076
 23. Rayner JE, Laino AM, Nufer KL, Adams L, Raphael AP, Menzies SW, Soyer HP. Clinical perspective of 3D total body photography for early detection and screening of melanoma. *Front Med (Lausanne)*. 2018 May 23;5:152.

- DOI: 10.3389/fmed.2018.00152
PMID: 29911103
PMCID: PMC5992425
24. Chuchu N, Takwoingi Y, Dinnes J, Matin RN, Bassett O, Moreau JF, Bayliss SE, Davenport C, Godfrey K, O'Connell S, Jain A, Walter FM, Deeks JJ, Williams HC; Cochrane skin cancer diagnostic test accuracy group. Smartphone applications for triaging adults with skin lesions that are suspicious for melanoma. *Cochrane Database Syst Rev.* 2018 Dec 4;12(12):CD013192.
DOI: 10.1002/14651858.CD013192
PMID: 30521685
25. Freeman K, Dinnes J, Chuchu N, Takwoingi Y, Bayliss SE, Matin RN, Jain A, Walter FM, Williams HC, Deeks JJ. Algorithm based smartphone apps to assess risk of skin cancer in adults: Systematic review of diagnostic accuracy studies. *British Medical Journal.* 2020;368:m127
Available:<http://dx.doi.org/10.1136/bmj.m127>, 2019
26. Dalimier E, Salomon D. Full-field optical coherence tomography: a new technology for 3D high-resolution skin imaging. *Dermatology.* 2012 May 1;224(1):84-92.

© Copyright (2024): Author(s). The licensee is the journal publisher. This is an Open Access article distributed under the terms of the Creative Commons Attribution License (<http://creativecommons.org/licenses/by/4.0>), which permits unrestricted use, distribution, and reproduction in any medium, provided the original work is properly cited.

Peer-review history:
The peer review history for this paper can be accessed here:
<https://prh.ikpress.org/review-history/11992>